ELSEVIER

Biophysical Chemistry 125 (2007) 425–434

Biophysical Chemistry

http://www.elsevier.com/locate/biophyschem

Interactions of chlorpromazine with phospholipid monolayers: Effects of the ionization state of the drug

Mónica Pickholz [a,*], Osvaldo N. Oliveira Jr. [b], Munir S. Skaf [a]

[a] *Instituto de Química, Universidade Estadual de Campinas-UNICAMP, C.P. 6154 Campinas, SP, 13083-970, Brazil*
[b] *Instituto de Física de São Carlos, Universidade de São Paulo, C.P. 780 São Carlos, SP, 13560-970, Brazil*

Received 14 June 2006; received in revised form 12 October 2006; accepted 16 October 2006
Available online 10 November 2006

Abstract

Molecular dynamics simulations have been performed to investigate the interactions between chlorpromazine (CPZ) and Langmuir monolayers of the zwitterionic dipalmitoylphosphatidylcholine (DPPC) and the anionic dipalmitoylphosphatidylglycerol (DPPG). Simulations for a fixed surface density and different charge states — neutral and protonated CPZ — were able to capture important features of the CPZ–phospholipid monolayer interaction. Neutral CPZ is predominantly found in the hydrophobic tail region, whereas protonated CPZ is located at the lipid–water interface. Specific interactions (hydrogen bonds) between protonated CPZ and the lipid head groups were found for both zwitterionic and anionic monolayers. We computed lipid tail order parameters and investigated the effects of the drug upon tail ordering. We also computed electrostatic surface potentials and found qualitative good agreement with experimental results.

Keywords: DPPC; DDPG; Chlorpromazine; Model membrane; Molecular dynamics; Monolayers

1. Introduction

The phenothiazine family of drugs has been shown to elicit a variety of neuroleptic effects. Chlorpromazine (CPZ), one of the best-known phenothiazines, is an antipsychotic agent used in the treatment of schizophrenia [1]. Numerous experiments on model membranes and monolayers have shown that CPZ interacts with the membrane phospholipids, especially with negatively charged ones [2,3]. The tricyclic ring structure of CPZ is hydrophobic, partitioning with relative ease into the bulk hydrocarbon phase of membrane bilayer systems, while the tertiary propylamine tail region of the drug is hydrophilic, interacting well with the polar headgroups of membrane bilayers [4]. The tertiary amines have p*K* values near the physiological pH, and consequently may occur both in charged (protonated) and uncharged forms while interacting with biological systems [5]. There is experimental evidence from lipid membrane studies that at physiological pH CPZ may remain protonated [6] and located preferably at the water–lipid interface [2,3]. Other experimental results indicate that CPZ may also penetrate into the acyl chain region of phospholipid membranes, affecting the acyl chain order [7] and lipid phase transition,[8] thus suggesting the prevalence of a non-charged solute.

Wisniewska and Wolnicka-Glubisz [9] have shown that the different forms of CPZ influence membranes unequally. When protonated, CPZ cannot easily penetrate into the membrane, and remains mainly at the interface or bilayer surface. The amino group of CPZ should be located around the phosphate atom of PC (phosphatidylcholine) and the volumous phenothiazine ring system may go deeper into the interfacial region. In contrast, neutral CPZ, which is the predominant species at pH = 9.0 and higher [6], can easily penetrate the membrane and is expected to be more evenly distributed within the hydrophobic parts of the membrane structure.

We have recently used molecular dynamics simulations to study interactions between neutral (unprotonated) CPZ and dipalmitoylphosphatidylcholine (DPPC), a zwitterionic phospholipid, in Langmuir monolayers [10]. The simulations carried out at different monolayer surface coverages, ranging from 50 to 80 $Å^2$ per lipid molecule, were able to capture important features of the CPZ–lipid interaction and monolayer ordering.

* Corresponding author.
E-mail address: monik@ifi.unicamp.br (M. Pickholz).

0301-4622/$ - see front matter © 2006 Elsevier B.V. All rights reserved.
doi:10.1016/j.bpc.2006.10.010

We found that neutral CPZ is preferentially located in the lipid tail region of the phospholipids, in little contact with the aqueous phase, and that its rigid ring orientation and tail conformation vary with lipid surface density. Neutral CPZ was found to promote ordering of the lipid tails for all surface densities considered because its presence reduces the effective surface area per lipid. For a dense monolayer (50 $Å^2$/lipid), CPZ induces a local distortion of the lipid tails in its immediate vicinity and the concomitant ordering of lipid tails further away from the solute. Other structural and dynamical properties were also discussed for neutral chlorpromazine.

In the present work, we extend our analysis to a cationic CPZ since, as already mentioned, the protonated form of the drug may also play an important role at membranes in biologically relevant contexts. Here, we shall focus on comparing the main effects of neutral and protonated CPZ (nCPZ and pCPZ, respectively) upon a zwitterionic DPPC monolayer and an anionic (fully deprotonated) dipalmitoylphosphatidylglycerol (DPPG) monolayer at the air/water interface at a fixed area per lipid of 70 $Å^2$. The main goals are: (1) to investigate comparatively how the different monolayers respond to the presence of the drug, i.e., the extent to which the lipid headgroup composition influences the effect of CPZ upon the membrane, (2) to investigate the effects of the ionization state of the drug, representing distinct pH conditions at the membrane, upon the structural features of the monolayers, and (3) to elucidate the contributions from the different molecular species to the electrostatic surface potential across the interfaces. To address these issues we have performed molecular dynamics (MD) simulations for various systems, including neat monolayers (free of CPZ), as well as DPPC and DPPG monolayers with neutral and protonated CPZ. Monolayers with a surface area of 70 $Å^2$ per lipid were chosen because the equilibrium distribution of the phosphate groups for DPPC and DPPG monolayers are similar at this surface coverage [11], and also because the experimental surface potential difference between neat and CPZ containing monolayers is well pronounced at this surface density [12].

In the next section, we describe the simulated systems and computational details. In Section 3 we present molecular geometry and partial atomic charges for describing pCPZ in the simulations. The main results and concluding remarks are presented in Sections 4 and 5, respectively.

2. Systems and simulation details

The simulated systems consist of a periodically replicated cell containing two monolayers with 36 lipids each, as shown in Fig. 1, with DPPG on the left and DPPC on the right, hereafter referred to as MG and MC, respectively. The monolayers are separated by a slab containing 4188 water molecules and 36 Na^+ counterions, included to compensate the charge of the anionic phospholipids. The aqueous phase is sufficiently thick to ensure negligible interactions between the two monolayers. The simulation geometry, shown in Fig. 1, is similar to that proposed by Feller et al. [13]. This strategy allows us to investigate the two monolayers simultaneously (MC and MG, with and without the drug). The system is effectively periodic in 3D and small interactions are expected across the z direction (normal to the interfaces) because of the large air region.

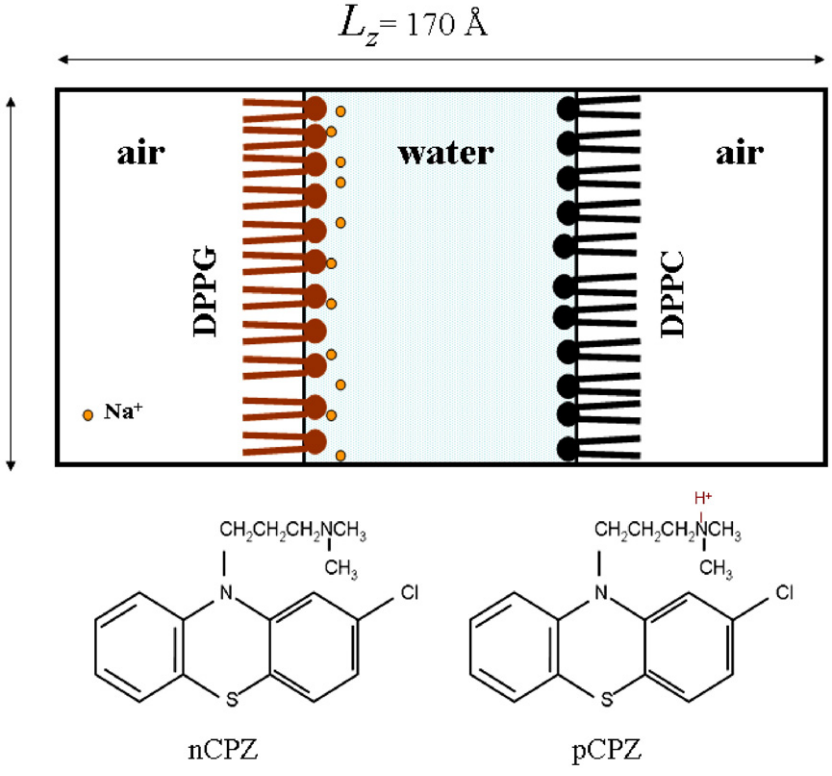

Fig. 1. Scheme of the simulation unit cell and molecular structures for neutral and protonated CPZ.

Simulations were carried out with either a neutral or a protonated CPZ in each monolayer to assess the effect of the drug's ionization state and also for neat monolayers for comparison purposes.

Simulations were performed for three distinct systems: 1) A pair of pure DPPG–DPPC opposing monolayers (MG/MC); 2) one neutral CPZ in each monolayer (nMG/nMC); and 3) one protonated CPZ in each monolayer (pMG/pMC). The charge of each protonated CPZ was compensated with a Cl^- counteranion. The CPZ molecules were initially placed at the lipid–water interface. The NAMD2 program [14] was used for the simulations with the PARAM27 CHARMM parameter set [15] and the water molecules were described by the TIP3P model [16]. The interaction parameters used for CPZ have been described in a previous article [10]. The ground state geometry of the neutral (unprotonated) and charged (protonated) chlorpromazine was optimized within the Density Functional Theory (DFT) using the B3LYP [17] functional and 631G* basis set. The partial atomic charges were obtained from a single point HF/6-31G* calculation using Gaussian [18] and the Merz–Singh–Kollman protocol [19]. The size of the simulation cell was kept constant to accommodate the 36 lipids on each interface, always keeping the sides $Lx=Ly=50.2$ Å (fixed area per lipid of 70 $Å^2$) and $Lz=170$ Å for every system considered. In our previous work [10], we have chosen $Lz=220$ Å to ensure that interactions across the z axis where negligible for each surface density considered at a fixed amount of water molecules. At the surface density of interest here $Lz=170$ Å suffices.

Classical MD simulations were performed with the system equilibrated at 323 K. Following standard procedures, the simulation of each system consisted of an equilibration period of about 3 ns (NVT ensemble), within which the CPZ molecules migrated to their preferential location relative to the membrane, followed by an unperturbed (NVE) 5 ns run. A multiple-time step algorithm, RESPA [20], was used with the shortest time step of 2 fs. During simulations, all intramolecular motions involving hydrogen atoms were frozen using SHAKE/RATTLE algorithms [21]. The short-range forces were computed using a cutoff of 11 Å with smooth switching and the long-range forces were taken into account by means of the particle mesh Ewald (PME) technique [22].

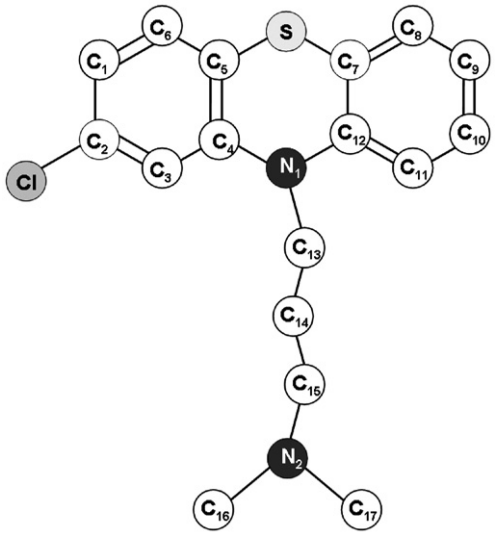

Fig. 2. Molecular structure of chlorpromazine and atom numbering.

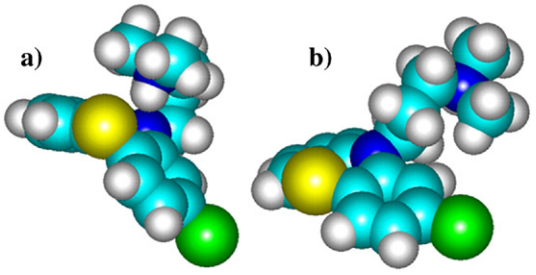

Fig. 3. Molecular conformations A and B of protonated CPZ, see text.

3. Chlorpromazine: geometry and charges

We carried out ground state geometry optimizations for neutral and protonated CPZ using DFT at the B3LYP/6-31G* level. The molecular structure of CPZ is shown in Fig. 2, along with the atom numbering scheme. The most stable geometry of the protonated CPZ (pCPZ) in gas phase (Fig. 3a) shows a *cis* conformation of its tail. In this conformation, hereafter named conformation A, the extra proton forms an intramolecular hydrogen bond with the central ring. However, subsidiary MD simulations showed that this conformation does not prevail in water at 323 K. In fact, in aqueous solutions the pCPZ tail is predominantly found in *trans* conformation. Therefore, in order to consider this in the parameterization of pCPZ atomic charges, we carried out a geometry optimization of the protonated molecule keeping selected dihedral angles at fixed values, resulting in a conformation referred to as B (see Fig. 3b). The values of these selected dihedral angles were taken from a fully optimized neutral complex of pCPZ-chlorine.

In Table 1 we show some selected dihedral angles for the optimized geometries obtained here. The partial atomic charges obtained from a single point HF/6-31G* calculation within the Merz–Singh–Kollman protocol [19] are shown in Table 2 for both conformations A and B, following the atom numbering of Fig. 2. Hydrogen charges were included below their corresponding heavy atom. Notice that A and B structures of pCPZ have different sets of partial charges.

Table 1
Selected dihedral angles (in degrees) of nCPZ and conformation A and B of pCPZ

	nCPZ	pCPZ (A)	pCPZ (B)
$C_3–C_4–N_1–C_{12}$	136.9	126.7	134.2
$C_3–C_4–N1–C_{13}$	−23.3	−18.9	−25.1
$C_4–N_1–C_{13}–C_{14}$	−63.4	−146.3	−61.8
$N_1–C_{13}–C_{14}–C_{15}$	−179.4	63.8	−163.9
$C_{13}–C_{14}–C_{15}–N_2$	−62.4	−67.3	−161.1
$C_{14}–C_{15}–N_2–C_{16}$	161.7	−76.6	−52.3
$C_{14}–C_{15}–N_2–C_{17}$	−73.7	157.5	−177.9

The atoms follow the numbering given in Fig. 2.

Table 2
Atomic charges in units of *e* (for numbering see Fig. 2)

	nCPZ	pCPZ (A)	pCPZ (B)
Cl	−0.123	−0.059	−0.092
C_1	−0.124	−0.098	−0.160
H_{C1}	0.166	0.167	0.177
C_2	0.054	−0.025	−0.015
C_3	−0.230	−0.101	−0.115
H_{C3}	0.190	0.131	0.107
C_4	0.295	0.016	0.252
C_5	−0.097	0.095	−0.040
C_6	−0.042	−0.178	−0.082
H_{C6}	0.150	0.191	0.173
S	−0.129	−0.166	−0.108
N_1	−0.486	−0.086	−0.599
C_7	−0.137	−0.029	−0.123
C_8	−0.003	−0.092	−0.024
H_{C8}	0.140	0.173	0.165
C_9	−0.294	−0.225	−0.258
H_{C9}	0.170	0.185	0.180
C_{10}	−0.068	−0.069	−0.091
H_{C10}	0.146	0.161	0.163
C_{11}	−0.331	−0.306	−0.315
H_{C11}	0.163	0.184	0.154
C_{12}	0.427	0.242	0.462
C_{13}	0.305	−0.536	0.261
H_{C13}	0.037/0.034	0.090/0.078	−0.008/0.003
C_{14}	−0.295	−0.070	0.062
H_{C14}	0.070/0.137	0.090/0.039	0.068/0.011
C_{15}	0.068	−0.053	−0.228
H_{C15}	0.065/0.051	0.112/0.102	0.132/0.154
N_2	−0.248	0.108	0.110
C_{16}	−0.421	−0.452	−0.400
H_{C16}	0.169/0.144/0.129	0.186/0.178/0.179	0.193/0.179/0.194
C_{17}	−0.212	−0.387	−0.341
H_{C17}	0.074/0.095/0.118	0.210/0.202/0.196	0.169/0.191/0.157
H^+		0.132	0.281

Despite the large energy difference between conformations A and B (A being nearly 12.5 kcal/mol lower due to the formation of an intramolecular hydrogen bond), conformation B is found from our simulations to be stabilized in membranes. We have carried out 5 ns simulations as described above for structures A and B in MG–MC monolayers. Results from these simulations show that structure B is stable since it remains in an open conformation 99% of the time. The picture is less clear for structure A, which alternates between open and closed conformations: pCPZ is found in an open conformation 35% and 43% in MC and MG, respectively. Here, we have defined open and closed conformation according to the distance between N1 and N2 nitrogens (Fig. 2). This separation is nearly 3 Å for structure A and larger than 4.0 Å for open structures [10]. Given that closed (intramolecular H-bond) and open (non-H bonded) conformations are nearly equally populated with the partial charges of A, which favors closed conformations in vacuo, we believe that open structure parameterizations such as B describe pCPZ more accurately under these conditions. Therefore, in this study we shall discuss mainly results obtained with structure B for the protonated form of CPZ. Only a few selected analyses are presented for pCPZ with structure A. Unless otherwise specified, reference to the pCPZ molecule stands for its conformation B.

4. Simulation results

4.1. Electron density profiles

The interfacial ordering of the system is evaluated here by means of the electron density profile (EDP) normal to the monolayer. The profiles were calculated by time averaging the net charge per 0.1 Å thick slabs, assuming a Gaussian distribution centered at the atomic positions with a width of approximately 2 Å. Fig. 4 shows EDPs for the three systems under investigation, with the electron density being plotted against the z coordinate, where $z=0$ corresponds to the system center located in the middle of the aqueous phase. Contributions to the electron density are shown for water, CPZ (amplified by a factor 5 for comparison purposes) and for monolayers MG (on the left) and MC (on the right). The Na^+ distribution is shown only for neat monolayers (amplified by a factor 2). Very similar distributions are found for the other cases, as we shall discuss shortly in terms of the partial charge distribution. A comparison

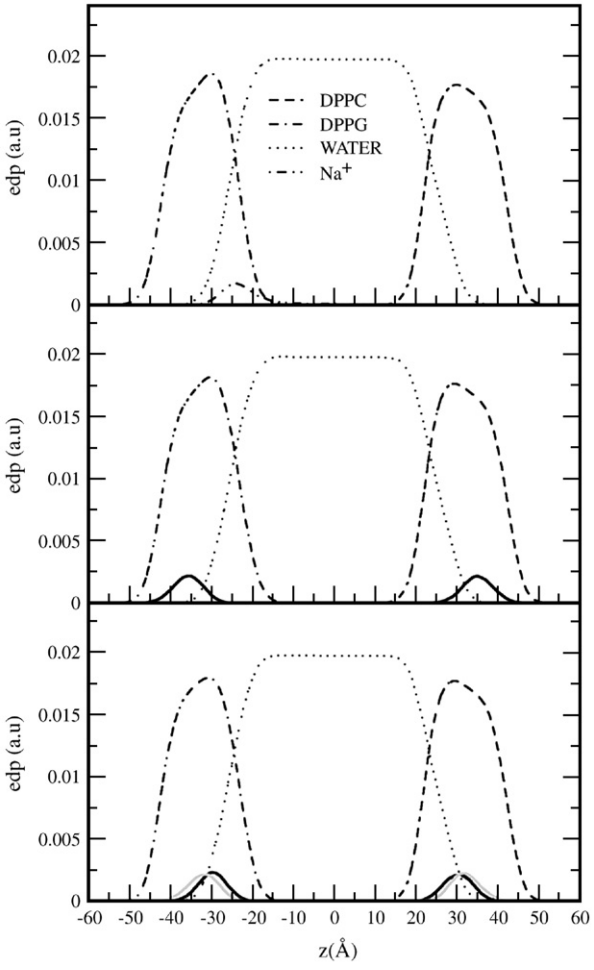

Fig. 4. EDP of the main system constituents: water (dotted lines), CPZ (solid lines; amplified 5 times for comparison purpose), Na^+ (amplified 2 times), and the monolayers MG (dashed dashed-dotted lines) and MC (dashed lines). a) Neat MG/MC monolayers; b) neutral CPZ in MG/MC monolayers; and c) protonated CPZ in MG/MC monolayers. The EDP of structure A of pCPZ is also included in this picture (grey lines).

of the profiles in panels a) through c) indicates that the overall lipid distribution is not significantly affected by either neutral or protonated CPZ, as previously seen for neutral CPZ interacting with DPPC at this surface density [10]. The EDP for water (dotted lines) drops from the bulk aqueous phase value to zero, as an essentially dry lipid tail region is reached passing through an intermediate complex lipid–water interfacial region in which the polar headgroups are hydrated.

Due to the complexity of the water/lipid interface, it is difficult to estimate its thickness precisely. Here, we estimate the interface thickness considering the function $f(z)$ defined as the product of the water and lipid electron density profiles [10]:

$$f(z) = \mathrm{EDP}_{\mathrm{water}}(z).\mathrm{EDP}_{\mathrm{lip}}(z).$$

$f(z)$ were fitted by a Gaussian function and the interface thickness, Δz, is taken as twice the Gaussian half-width. Although somewhat arbitrary, this measure turned out quite robust for different monolayers. The estimated values for Δz are shown in Table 3. The interface thickness remains nearly unaltered ($\sim$ 13.0 Å) for MC monolayers upon addition of either nCPZ or pCPZ, whereas for MG monolayers Δz increases a little in the presence of the drug, especially the neutral species. Results depicted in Fig. 4b show that neutral chlorpromazine is essentially solvated in the dry region for both monolayers, consistent with the molecular picture inferred from scanning calorimetric measurements [23] and our previous findings for DPPC lipid monolayers [10,24]. In contrast, protonated CPZ (Fig. 4c) is predominantly found in the extended lipid–water interface for both MG and MC monolayers, which is also consistent with ESR data [9]. In order to illustrate the effects of the conformation of pCPZ upon the density profiles, we have also included the EDP corresponding to the structure A of pCPZ (Fig. 4c). One can see that structure A pCPZ, being less polar than conformation B, partitions slightly away from the polar interface towards the lipid tail region. The overall distributions of lipids and water molecules are essentially the same for A and B pCPZ.

Further details about the CPZ orientation can be obtained by analyzing the distribution of its main groups, depicted in Fig. 5 for neutral (top panels) and protonated (middle and bottom panels) CPZ molecules. Separate group contributions to the EDPs are given for the tricyclic rigid ring structure and the tertiary propylamine tail for MG and MC monolayers. The overall lineshape of the distribution (not the mean location) of CPZ appears to be little affected by its charge state or lipid type, zwitterionic DPPC or anionic DPPG, and is somewhat sharper for protonated CPZ in structure B (bottom panels). However, the distributions of the rigid ring and tail structures differ between neutral and protonated CPZ. For nCPZ, there is a broad distribution for both ring and tail groups, with distribution

Table 3
Interfaces thickness (in Å) obtained from simulations

	MC	MG
Neat	13.1	12.2
nCPZ	13.3	13.4
pCPZ	12.8	12.8

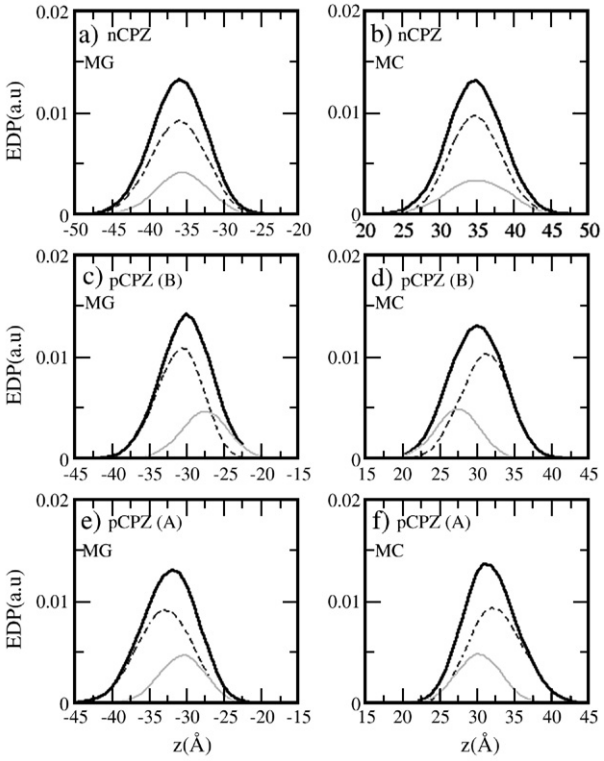

Fig. 5. Total and partial contributions to EDPs of neutral (top) and protonated CPZ (middle: structure B; bottom: structure A) in MG (left) and MC (right) monolayers. The total EDP of CPZ are shown in solid lines and the rigid ring and tail group contributions are depicted in dashed and dotted lines, respectively.

maxima near each other suggesting an orientational disorder of the molecule. In contrast, for pCPZ there is a different preferential region for each group: The tail makes deeper incursions into the aqueous region than does the rigid ring, suggesting that specific interactions between CPZ and both kinds of phospholipid heads may be taking place.

The possibility of such specific interaction is further examined by comparing data for DPPC (zwitterionic) and DPPG (anionic) in terms of the relative position between the pCPZ tail and the phosphate group that is common to both phospholipids. The radial distribution function, $g(r)$, between the nitrogen proton of pCPZ (structure B) and the phosphate oxygens for both phospholipid species are shown in Fig. 6. A sharp first peak located at $\sim$ 1.6 Å, characteristic of hydrogen (H)-bonding [25], is observed for both monolayers (MG and MC). As an example of the specific interactions found for these systems, Fig. 7 shows two MD snapshots illustrating typical H-bonds between pCPZ and the lipid phosphates for MG (panel A) and MC (panel B), in which only the drug and the relevant lipid molecule are shown. When conformation A for pCPZ is used, only a weak structure in the radial distribution function between the A-pCPZ proton and the phosphate oxygens appears around 1.8 Å for DPPG and essentially no short distance structure for DPPC. The lipid–drug interaction obtained for structure B seems to be more consistent with recent NMR measurements [26], which have shown specific interactions between CPZ and phosphate groups of lipid bilayers, especially for SDPS (1-stearoyl-2-docosahexaenoylsn-glyerco-3-phosphocholine) bilayers.

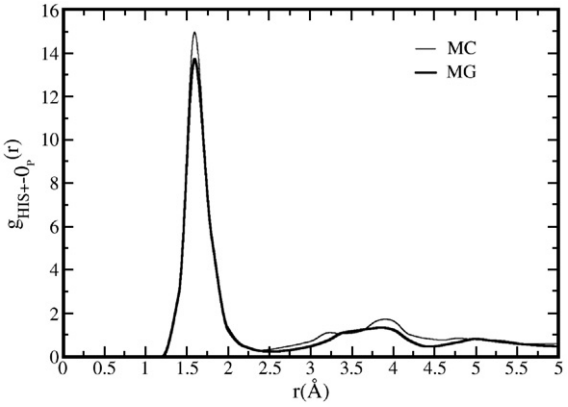

Fig. 6. Radial distribution function between the pCPZ's H^+ site and the phosphate oxygens for DPPC and DPPG phospholipids.

4.2. Lipid tail ordering

The lipid tail order parameter is a standard quantity to evaluate the structural order of acyl chains in lipid bilayers, which can be obtained from deuterium NMR measurements. The experimental order parameter, $S_{CD}=-{}^1/_2\, S_{mol}$, is derived from the measured residual quadrupole splitting $\Delta\acute{\imath}=(3/4)(e^2qQ/h)S_{CD}$ [27]. In MD simulations, it can be determined by :

$$S_{mol}=\frac{1}{2}3\cos^2{}_n-1,$$

where $_n$ is the angle between the normal to the bilayer and the normal to the plane defined by two carbon–deuterium (C–D) bonds in a deuterated *n*-methylene group of the lipid acyl chain. $S_{mol}\approx 1$ indicates that the chains are all *trans* and perpendicular to the bilayer plane, $S_{mol}\approx 0.5$ indicates that they are all *trans* and parallel to the plane, and $S_{mol}\approx 0$ corresponds to random orientation. The order parameter is related to the tilt angle of the chains and to *trans-gauche* distribution of chain dihedrals, but the relationship is indirect [28]. Fig. 8 shows the S_{CD} order parameters for all lipid methylene groups for MC (panel a) and MG (panel b) monolayers with and without the drug. Rough error bar estimates were obtained by dividing the trajectories into blocks of varying lengths. As already pointed out by de Vries et al. [29], 3 ns simulations are sufficiently long to yield qualitatively consistent results for S_{CD}. The C_{H2} groups are numbered consecutively from 2 to 15. The carbonyl and CH_3 carbons are labeled 1 and 16, respectively. Overall, the results are typical of phospholipid monolayers [11] showing higher orientational order (larger S_{CD}) for the methylene groups located in the middle of the lipid tails. The magnitudes of S_{CD} for DPPC monolayers are similar to those reported by Kaznessis et al. [11], but for DPPG our systems seem to be somewhat more disordered. The drug introduces relatively small changes in the tail ordering. The effects are slightly more apparent for neutral CPZ, which induces some ordering of the lipid tails in both monolayers. This is consistent with nCPZ being preferentially located in the lipid tail region, thus contributing to a reduction of the effective surface area per lipid [10]. In the presence of protonated CPZ the order parameters are essentially indiscernible within the error bars from that of the neat monolayers.

4.3. Charge density and surface potential

Mean charge densities, $\rho(z)$, for each molecular species on *xy*-plane slices of the periodic box as functions of *z* were obtained by averaging over the trajectories. In Fig. 9a we compare the charge density of the Na^+ counterions for the three cases: MG/MC (CPZ-free), nMG/nMC, and pMG/pMC monolayers. The lipid–water interface boundaries were schematically drawn, as determined above. The distributions of sodium ions are very similar for all

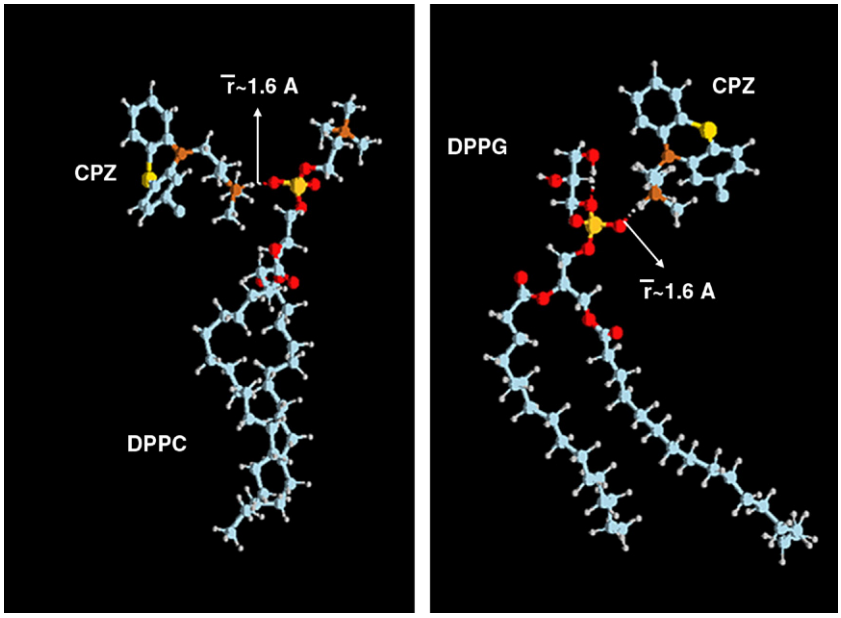

Fig. 7. MD snapshot showing typical H-bonding between the lipid and *p*-CPZ. The solvent and remainder lipid molecules were omitted for visualization purposes. a) DPPC; b) DPPG.

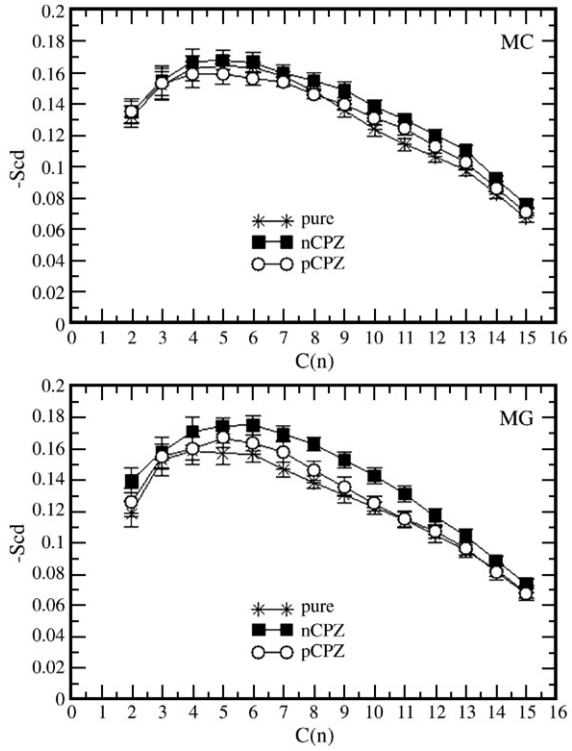

Fig. 8. Order parameters ($-S_{CD}$) as a function of the position of the carbon atoms along the hydrocarbon chain of DPPC and DPPG.

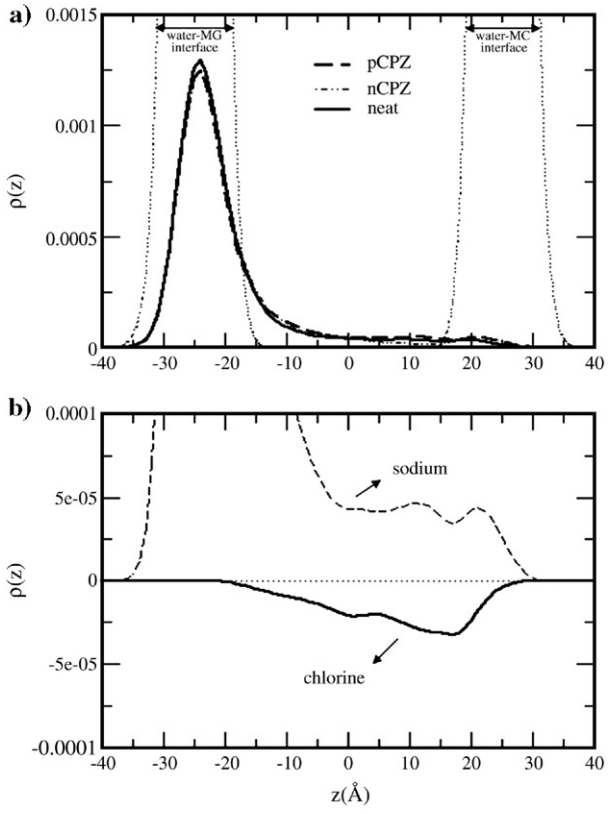

Fig. 9. a) Sodium counterion partial charge distribution; b) sodium and chlorine distribution in monolayers with pCPZ.

three cases: The Na^+ are predominantly located within the MG–water interface, a small fraction of the cations are found in the aqueous phase and in the MC–water interface, whereas the hydrophobic regions of the monolayers are totally depleted of sodium. The average number of sodium ions, N_{Na+}, present in the MG–water interface is estimated by integrating $\rho_{Na+}(z)$ up to $z=-15$ Å. For the neat and nCPZ monolayers, N_{Na+} is essentially the same (30.6 and 30.5, respectively). For pCPZ monolayers, N_{Na+} drops to 29.5, indicating that one of the interfacial counterions is being replaced by the positively charged CPZ at the MG–water interface.

Fig. 9b focuses on the aqueous regions of the Na^+ and Cl^- charge distributions. Both ions are found in the water and water–lipid interfaces with no access to the hydrophobic tail regions. No Cl^- is found in the MG–water interface due to Coulomb repulsion between the chlorine and the anionic lipids. The region of highest Cl^- density lies near the range of preferential location of the pCPZ molecule in the MC monolayer ($z\sim 18$ Å). Since an appreciable fraction of the Na^+ and Cl^- counterions are solvated in the bulk of the aqueous phase, the electrical properties of the solvent are expected to differ from that of pure water.

The electrostatic potential profile, $\Delta\phi(z)$, across the interface arising from the non-uniform distribution of dipoles is calculated by a double integration of Poisson's equation:

$$(z) = (z) - () = -\frac{1}{0\,0}^{z} z_0^z(z)z,$$

where $\rho(z)$ is the time averaged charge density from 0.1 Å bins.

First, let us focus on the potential profile across the interface normal. Fig. 10 shows the potential profile, $\Delta\phi(z)$, for neat MC monolayers and with CPZ (neutral and protonated). Depicted are the results for the total surface potential (non−solid lines) and the contributions from the DPPC lipids (solid lines) for the three MC systems considered. As discussed by Skibinsky et al., [30] the drop in the potential profile as one goes from the lipid tail region towards more polar environments results from a large positive contribution from the lipid headgroups and a negative water contribution (not shown). The total profile is little affected

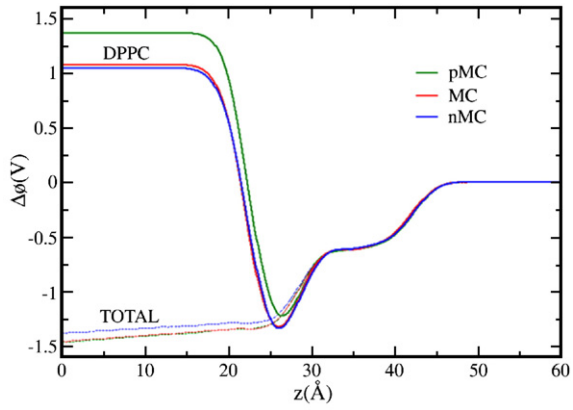

Fig. 10. Potential for DPPC lipids (solid lines) and total (dashed lines), for neat MC (red), nCPZ/MC (blue) and pCPZ/MC (green). (For interpretation of the references to colour in this figure legend, the reader is referred to the web version of this article.)

by the presence of the drug, consistent with experimental results [12], according to which CPZ does not cause appreciable changes in the surface pressure and surface potential isotherms of the zwitterionic DPPC monolayers at low drug concentrations. However, the lipid contribution to the surface potential is clearly affected by the presence of pCPZ since it increases by 0.3 V relative to the lipid contributions in MC and nMC monolayers. This increase is compensated by the rest of the moieties in the system, since the total potential does not change appreciably by the addition of pCPZ. Such an increase in the lipid contribution to the potential suggests lipid conformational changes in presence of pCPZ.

In Fig. 11, we examine the surface potential profiles for the MG monolayers. Results are shown for the combined lipid plus Na^+ profiles (solid lines), water contributions (dashed lines), and total potential profiles (dotted lines). The total potential is almost unaffected by the drug in either ionization states (insert to Fig. 11). Similar to the MC systems, this feature stems from the cancellation of a large positive contribution of the anionic lipids and their counterions (ranging from ~ 8 to ~ 11 V) and negative contributions from water. The effects from the drug on the aqueous contributions to the potential profile, however, turned out somewhat different. Fig. 11 shows that nCPZ/MG and pCPZ/MG exhibit nearly equal water potentials and both are less negative than the corresponding potential in neat DPPG monolayer at this surface coverage. The protonated CPZ increases the lipids plus Na^+ potential relative to that of the neat MG monolayer, whereas neutral CPZ reduces this potential.

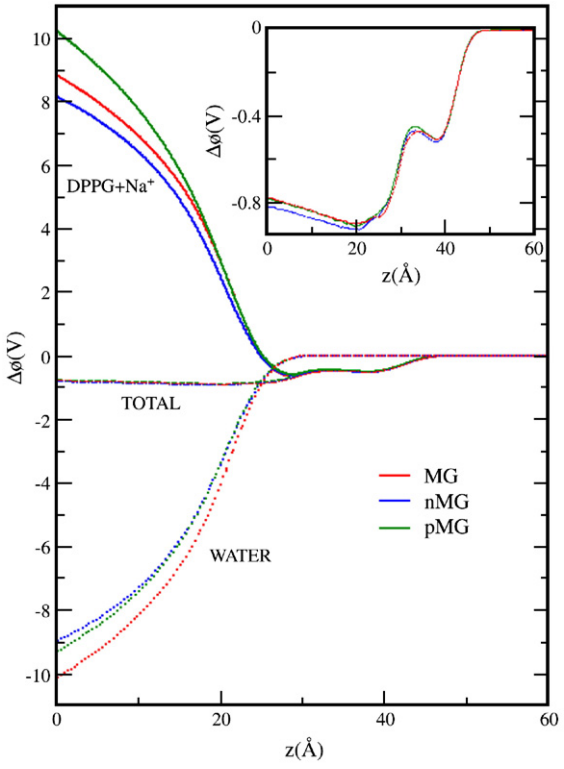

Fig. 11. Potential for DPPG lipids plus their counterions (solid), water (dotted), and total (dashed), for neat MG, nCPZ MG and pCPZ MG.

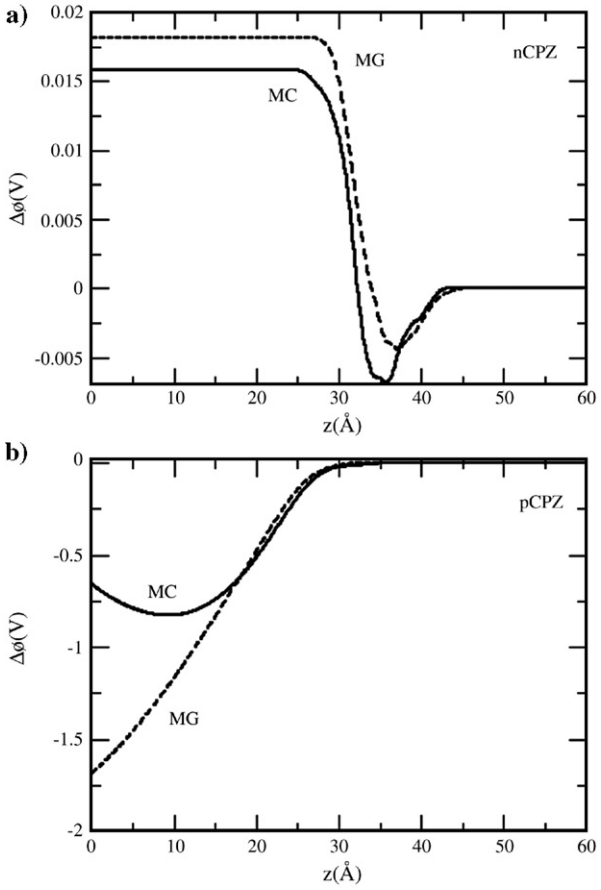

Fig. 12. Potential of nCPZ and pCPZ plus Cl^-, (a) and (b) panels respectively, for MC (solid lines) and MG (dashed lines) monolayers.

The partial potential profile from the drug alone (nCPZ) and the combined potential from pCPZ plus its chlorine counterion in both types of monolayers are depicted in Fig. 12. Neutral CPZ displays very small, positive potentials in MC and MG. The potential profile for the neutral, solvent separated, ionic pair pCPZ/Cl^- depends on lipid type. For the MC monolayer (Fig. 12a), in which the chlorine ion and pCPZ are both found roughly in the same approximate vicinity relative to the interface (cf. Figs. 4 and 9), the pCPZ/Cl^- combined profile passes through a local minimum of nearly −0.8 V at 10 Å. This distance corresponds roughly to the average separation between the drug and its counterion in the zwitterionic monolayer, suggesting that the calculated potential drop of 0.8 V arises from the dipolar contribution of the solvent separated pCPZ/Cl ionic pair. Moreover, the change in the sign of the potential derivative indicates a reversal of the electric field created by the drug and its counterion at $z \sim 10$ Å. For the DPPG monolayer, in contrast, pCPZ and Cl^- are located far apart from each other (the drug sits at the MG/water interface, Fig. 4, while Cl^- is predominantly located at the MC/water interface, Fig. 9) and the monotonic potential indicates no reversal of the ionized drug plus counterion electric field component along the interface normal in the range shown in Fig. 12.

Correspondence with experimentally measured surface potential is made by considering the variation of $\Delta\phi(z)$ as one goes from vacuum to the bulk aqueous phase. Let us define the

Table 4
Surface potential from simulations, ΔV^{sim}, computed for 70 Å^2/lipid and CPZ concentration of approximately 0.03 mol/L

	ΔV^{sim} (V)
MC	0.96(3)
pMC	0.98(4)
nMC	0.84(3)
MG	0.27(3)
pMG	0.30(5)
nMG	0.32(4)

surface potential drop, $\Delta\Delta\phi$, as the total potential difference between aqueous and vacuum phases:

$$= _{\text{total}}(z =) - _{\text{total}}(z = 0).$$

It is possible to correlate this quantity with the experimental surface potential, ΔV, by:

$$V^{\text{sim}} = + _{\text{water}}$$

where Φ_{water} is the neat water/vapor surface potential in absence of the monolayer and ΔV^{sim} is the surface potential obtained from simulations. This relationship accounts for the fact that the experimental surface potential is measured relative to the pure water/air interface value. The value of Φ_{water} for the TIP3P model of water is reported to be −500 mV [31,32] and we use this value to estimate ΔV^{sim}. It is well-known that the interfacial potential of water, Φ_{water}, cannot be measured directly and experimental propositions for its magnitude — even for its sign — vary greatly [33]. Table 4 shows the surface potential, ΔV^{sim}, from our simulations. Neat MC and MG monolayers simulated surface potential are 0.96 V and 0.27 V, respectively. The surface potentials of MG neat monolayer are significantly lower than those of MC. The difference in surface potential between MC and MG monolayers is ~ 0.64 V from simulations and ~ 0.52 V from experiments (taken from Ref. [12]). This result is consistent with the fact that the zwitterionic lipid has a large permanent dipole moment (P–N group), whereas the head groups of DPPG are efficiently screened by both penetration of counterions and water around the lipid polar groups. The surface potential is barely increased in the presence of pCPZ for both monolayers. This seems to be in good experimental agreement for MC monolayers, which are almost unaffected by CPZ [12]. According to simulations, CPZ has practically no effect on the surface potential for DPPG monolayers as well, in disagreement with experiments, which report an approximately 0.15 V increase in ΔV at CPZ concentration 0.047 M [12]. The reasons for this discrepancy are not entirely clear to us. However, significant quantitative differences are not unexpected if simulated and actual reference solutions differ.

5. Concluding remarks

MD simulations were used to investigate the effects from the ionization state of CPZ upon its location, relative orientation, and distribution in a zwitterionic DPPC monolayer and an anionic DPPG monolayer. For simulations in the fluid lamellar phases at 70 Å^2 per lipid and 323 K, neutral CPZ was essentially solvated into the dry region of zwitterionic as well as anionic monolayers, showing no specific interactions. Protonated CPZ, on the other hand, was predominantly found in the lipid headgroup–water interface, consistent with NMR data. Also, specific interaction in the form of H-bonds could be identified between the charged group of protonated CPZ and the phospholipid phosphate. An analysis of the methylene group order parameters revealed that the drug introduces small changes (if any) in the tail ordering, being slightly more apparent for neutral CPZ, which induces ordering of the lipid tails in both monolayers. Our calculations of the electrostatic surface potentials pointed to a small increase in the surface potential of both types of monolayers upon addition of CPZ, in qualitative agreement with experimental results. However, for DPPG, the potential increase is much smaller than experimentally observed for 70 Å^2/lipid monolayers at supposedly similar thermodynamic conditions.

Effects from CPZ on DPPC/DMPC (1,2-dimyristoyl-*sn*-glycero-3-phosphocholine) liposomes, which carry no net charge, were found to be very small [2] and this suggests a small degree of CPZ interaction with these uncharged phospholipids. However, we observed in this work that protonated CPZ interacts via hydrogen bonds both with zwitterionic and anionic lipid monolayers. In zwitterionic phospholipids, this interaction is in competition with the mutual attraction between the highly polar P–N groups of distinct lipids. It depends on solute concentration and surface density, and may be involved in the cooperative phenomena and solute clustering observed experimentally in these systems [34]. The force field and system settings used here seem robust to describe the main properties of CPZ in lipid monolayers. However, one needs to bear in mind that in our previous study [10] and here, we employed a CPZ concentration of 0.027 M, at which there may be a tendency of CPZ to self aggregate [24]. It would be interesting to concentrate efforts towards simulating much larger systems, with multiple copies of the solute molecule, in order to investigate the formation of aggregates and their putative effects on the lipid monolayers.

Acknowledgments

This work was supported by the Brazilian agencies FAPESP (03/09361-4 to M.S. and 03/07404-8 to M.P.) and CNPq (401913/2003-1 and 479800/2004-9 to M.S.).

References

[1] J.Y. Chen, L.S. Brunauer, F.C. Chu, C.M. Helsel, M.M. Gedde, W.H. Huesti, Selective amphipathic nature of chlorpromazine binding to plasma membrane bilayers, Biochim. Biophys. Acta 1616 (2003) 95–105 (1616).
[2] W. Nerdal, S.A. Gundersen, V. Thorsen, H. Hoiland, H. Holmsen, Chlorpromazine interaction with glycerophospholipid liposomes studied by magic angle spinning solid state (13)C-NMR and differential scanning calorimetry, Biochim. Biophys. Acta 1464 (2000) 165–175.
[3] A.V. Agasøster, L.M. Tungodden, D. Cejka, E. Bakstad, L.K. Sydnes, H. Holmsen, Chlorpromazine-induced increase in dipalmitoylphosphatidylserine surface area in monolayers at room temperature, Biochem. Pharmacol. 61 (2001) 817–825.
[4] Y. Kuroda, K. Kitamura, Intra- and intermolecular proton–proton nuclear Overhauser effect studies on the interactions of chlorpromazine with lecithin vesicles, J. Am. Chem. Soc. 106 (1984) 1–6.

[5] W. Caetano, M. Tabak, Interaction of chlorpromazine and tifluoperzine with anionic Sodium Dodecyl Sulfate (SDS) micelles: electronic absorption and fluorescence studies, J. Colloid Interface Sci. 225 (2000) 69–81.
[6] H. Ahyayauch, F.M. Goñi, M. Bennouna, pH-dependent effects of chlorpromazine on liposomes and erythrocyte membranes, J. Liposome Res. 13 (2003) 147–155.
[7] J. Römer, M.H. Bickel, Biochem. Pharmacol. 28 (1979) 799.
[8] A. Jutila, T. Söderlund, A.L. Pakkanem, M. Huttunen, P.K.J. Kinnunen, Comparison of the effects of clozapine, chlorpromazine, and haloperidol on membrane lateral heterogeneity, Chem. Phys. Lipids 112 (2001) 151–163.
[9] A. Wisniewska, A. Wolnicka-Glubisz, ESR studies on the effect of cholesterol on chlorpromazine interaction with saturated and unsaturated liposome membranes, Biophys. Chem. 111 (2004) 43–52.
[10] M. Pickholz, O.N. Oliveira Jr., M.S. Skaf, Molecular dynamics simulations of neutral chlorpromazine in zwitterionic phospholipids monolayers, J. Phys. Chem., B 110 (2006) 8804–8814.
[11] Y.N. Kaznessis, S. Kim, R.G. Larson, Simulations of zwitterionic and anionic phospholipid monolayers, Biophys. J. 82 (2002) 1731–1742.
[12] A.A. Hidalgo, W. Caetano, M. Tabak, O.N. Oliveira Jr., Interaction of two phenothiazine derivatives with phospholipid monolayers, Biophys. Chem. 109 (2004) 85–104.
[13] S.E. Feller, Y. Zhang, R.W. Pastor, Computer simulation of liquid/liquid interfaces. II. Surface tension-area dependence of a bilayer and monolayer, J. Chem. Phys. 103 (1995) 10267–10276.
[14] L. Kalé, R. Skeel, M. Bhandarkar, R. Brunner, A. Gursoy, N. Krawetz, J. Phillips, A. Shinozaki, K. Varadarajan, K. Schulten, NAMD2: greater scalability for parallel molecular dynamics, J. Comp. Physiol. 151 (1999) 283.
[15] B.R. Brooks, R.E. Bruccoleri, B.D. Olafson, D.J. States, S. Swaminathan, M. Karplus, J. Comp. Chem. 4 (1983) 187.
[16] W.L. Jorgensen, J. Chandrasekhar, J.D. Madura, Comparison of simple potential functions for simulating liquid water, J. Chem. Phys. 79 (1983) 926–935.
[17] A.D. Becke, J. Chem. Phys. 98 (1993) 5648.
[18] M.J. Frisch, G.W. Trucks, H.B. Schlegel, G.E. Scuseria, M.A. Robb, J.R. Cheeseman, V.G. Zakrzewski, J.J.A. Montgomery, R.E. Stratmann, J.C. Burant, S. Dapprich, J.M. Millam, A.D. Daniels, K.N. Kudin, M.C. Strain, O. Farkas, J. Tomasi, V. Barone, M. Cossi, R. Cammi, B. Mennucci, C. Pomelli, C. Adamo, S. Clifford, J. Ochterski, G.A. Petersson, P.Y. Ayala, Q. Cui, K. Morokuma, D.K. Malick, D. Rabuck, K. Raghavachari, J.B. Foresman, J. Cioslowski, J.V. Ortiz, B.B. Stefanov, G. Liu, A. Liashenko, P. Piskorz, I. Komaromi, R. Gomperts, R.L. Martin, D.J. Fox, T. Keith, M.A. Al-Laham, C.Y. Peng, A. Nanayakkara, C. Gonzalez, M. Challacombe, P.M.W. Gill, B. Johnson, W. Chen, M.W. Wong, J.L. Andres, C. Gonzalez, M. Head-Gordon, E.S. Replogle, J.A. Pople, GAUSSIAN98 (Revision A.7), Gaussian Inc., Pittsburgh, PA, 1998.
[19] (a) U.C. Singh, P.A. Kollman, An approach to computing electrostatic charges for molecules, J. Comput. Chem. 5 (1984) 129–145;
(b) P. Cieplak, P.A. Kollman, On the use of electrostatic potential derived charges in molecular mechanics force fields. The relative solvation free energy of *cis*- and *trans*-*N*-methyl-acetamide, J. Comput. Chem. 12 (1991) 1232–1236.
[20] M.E. Tuckerman, B.J. Berne, G.J.J. Martyna, Reversible multiple time scale molecular dynamics, Chem. Phys. 97 (1992) 1990–2001.
[21] H.C. Andersen, Rattle: a "velocity" version of the shake algorithm for molecular dynamics calculations, J. Comput. Phys. 52 (1983) 24–34.
[22] T. Darden, D. York, L.J. Pedersen, Particle mesh Ewald: an N·log(N) method for Ewald sums in large systems, J. Chem. Phys. 98 (1993) 10089–10092.
[23] P.P. Constantinides, N. Inouchi, T.R. Tritton, A.C. Sartorelli, J.M. Sturtevant, A scanning calorimetric study of the interaction of anthracyclines with neutral and acidic phospholipids alone and in binary mixtures, J. Biol. Chem. 261 (1986) 10196–10203.
[24] We point out that the partial charges for CPZ were obtained using ChelpG in Ref. [10] and the MSK protocol in the present work. The fact that the CPZ electron density profiles in the DPPC monolayer reported here and in Ref. 10 at 70 $Å^2$/lipid agree suggests that both parameterization of the solute partial charges are reasonable and robust for the properties investigated here.
[25] B.M. Ladanyi, M.S. Skaf, Computer simulation of hydrogen-bonding liquids, Annu. Rev. Phys. Chem. 44 (1993) 335–368.
[26] S. Chen, A.U. Gjerde, H. Holmsen, W. Nerdal, Inportance of polyunsaturated acyl chains in chlorpromazine interaction with phosphatidylserines: a 13C and 31P solid-state NMR study, Biophys. Chem. 117 (2005) 101–109.
[27] A. Seelig, J. Seelig, The dynamic structure of fatty acyl chains in a phospholipid bilayer measured by deuterium magnetic Resonance, J. Biochem. 13 (1974) 4839–4845.
[28] L. Koubi, M. Tarek, M.L. Klein, D. Sharf, Distribution of halothane in a dipalmitoyl phosphatidylcholine bilayer from molecular dynamics calculations, Biophys. J. 78 (2000) 800–811.
[29] A.H. de Vries, I. Chandrasekhar, W.F. van Gunsteren, P.H. Hünenberger, Molecular dynamics simulations of phospholipid bilayers: influence of artificial periodicity, system size, and simulation time, J. Phys. Chem B, 109 (2005) 11643–11652.
[30] A. Skibinsky, R.M. Venable, R.W. Pastor, A molecular dynamics study of the response of lipid bilayers and monolayers to trehalose, Biophys. J. 89 (2005) 4111–4121.
[31] G. Lamoureux, A.D. MacKerell Jr., B. Roix, A simple polarizable model of water based on classical drude oscillators, J. Chem. Phys. 119 (2003) 5185–5197.
[32] S.E. Feller, R.W. Pastor, A. Rojnuckarin, S. Bogusz, B.R. Brooks, Effect of electrostatic force truncation on interfacial and transport properties of water, J. Phys. Chem. 100 (1996) 17011–17020.
[33] M. Paluch, Electrical properties of free surface of water and aqueous solutions, Adv. Colloid Interface Sci. 84 (2000) 27–45.
[34] E. Wajneberg, M. Tabak, P.A. Nussenzveig, C.M. Lopes, S.R. Louro, pH-dependent phase transition of chlorpromazine micellar solutions in the physiological range, Biochim. Biophys. Acta 944 (1988) 185–190.